Synthesis and Structures of Strained, Neutral [d^7] and Cationic [d^6] Hydrocarbon-Bridged [*n*]Cobaltocenophanes (*n* = 2, 3)

Ulrich F. J. Mayer, Jonathan P. H. Charmant, James Rae, and Ian Manners*

School of Chemistry, University of Bristol, Cantock's Close, Bristol, BS8 1TS, U.K.

Received September 21, 2007

The first neutral and paramagnetic [*n*]cobaltocenophanes Co(η^5-$C_5H_4)_2(CH_2)_2$ (**5**) and Co(η^5-$C_5H_4)_2(CH_2)_3$ (**6**) with sterically undemanding hydrocarbon bridges were prepared by the reaction of $CoCl_2$ with the corresponding ligand precursor $(LiC_5H_4)_2(CH_2)_n$ (n = 2 for **5**; n = 3 for **6**) in THF. In order to analyze the ring strain present, the molecular structures of **5** and **6** were determined using single-crystal X-ray diffraction. The neutral, paramagnetic 19-valence-electron [2]cobaltocenophane **5** is substantially distorted from metallocene-type geometry (tilt angle α: 27.1(4)°) and therefore highly strained, whereas [3]cobaltocenophane **6** is only moderately distorted (α: 12.0(11)°). Both **5** and **6** were readily oxidized with NH_4Cl in the presence of atmospheric oxygen to form the corresponding cationic [*n*]cobaltocenophane salts [Co(η^5-$C_5H_4)_2(CH_2)_n^+$][A$^-$] **7** and **8** (n = 2) and **9** (n = 3). Compound **7** (A = Cl) was isolated by means of extraction into CH_2Cl_2, whereas **8** and **9** were isolated by phase precipitation from aqueous solutions of $NaPF_6$. The X-ray analysis for cationic, diamagnetic, 18-valence-electron [2]cobaltoceniumphane **7** revealed substantially less distortion from metallocene-type geometry (tilt-angle α: 21.4(2)°) compared to paramagnetic 19-valence-electron compound **5**. In order to examine the electronic structures of **5**, **6**, **8**, and **9**, solution UV–vis spectra were recorded, and these reflected the increasing distortion as a result of the introduction of progressively shorter *ansa*-bridges. Cyclic voltammetric analysis of **8** and **9** in CH_2Cl_2 revealed that each cobaltoceniumphane exhibits a one-electron reduction, whereby redox potentials $E°$ appeared to vary as a function of the tilt angle.

Introduction

Metallopolymers with transition metals in the main chain are of growing interest due to their potential as easily processable materials with intriguing physical (e.g., redox, magnetic, electrical, and photophysical) and chemical (e.g., catalytic and preceramic) properties.[1] Ferrocenophanes with a variety of bridging moieties are well-studied, and their reactivity is broadly understood.[2] The transformation of strained [1]ferrocenophanes[3] and hydrocarbon-bridged [2]ferrocenophanes[4] (**1**) into polyferrocenes (**2**) via ring-opening polymerization (ROP) has been well-explored[5] (Scheme 1). In particular, well-defined architectures with low polydispersity can be achieved using the mild conditions of living anionic polymerization,[6a,b] including the recently developed photolytic ROP[6c], method.

Scheme 1. Ring-Opening Polymerization (ROP) of Ferrocenophanes 1

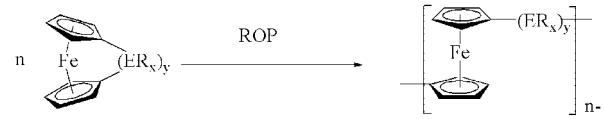

1 **2**

* Corresponding author. E-mail: Ian.Manners@bristol.ac.uk.

(1) (a) Abd-El-Aziz A. S., Carraher, C. E., Jr., Pittman, C. U., Jr., Sheats J. E., Zeldin M., Eds. *Transition Metal-Containing Polymers*; John Wiley & Sons, Inc.: Hoboken, NJ, 2006. (b) Whittell, G. R.; Manners, I. *Adv. Mater.* **2007**, *19*, 3439. (c) Manners, I. *Science* **2001**, *294*, 1664. (d) Marin, V.; Holder, E.; Hoogenboom, R.; Schubert, U. S. *Chem. Soc. Rev.* **2007**, *36*, 618. (e) Williams, K. A.; Boydston, A. J.; Bielawski, C. W. *Chem. Soc. Rev.* **2005**, *36*, 729. (f) Liu, L.; Wong, W. Y.; Poon, S. Y.; Shi, J. X.; Cheah, K. W.; Lin, Z. *Chem. Mater.* **2006**, *18*, 1369. (g) Abd-El-Aziz, A. S. *Macromol. Rapid Commun.* **2002**, *23*, 995. (h) Korczagin, I.; Lammertink, R. G. H.; Hempenius, M. A.; Golze, S.; Vancso, G. J. *Adv. Polym. Sci.* **2006**, *200*, 91.

(2) For recent reviews on strained metallocenophanes and related organometallic rings containing π-hydrocarbon ligands and transition metal centers and their transformation into polymetallocenes see: (a) Herbert, D. E.; Mayer, U. F. J.; Manners, I. *Angew. Chem., Int. Ed.* **2007**, *46*, 5060. (b) Bellas, V.; Rehahn, M. *Angew. Chem., Int. Ed.* **2007**, *46*, 5082.

(3) (a) Foucher, D. A.; Tang, B. Z.; Manners, I. *J. Am. Chem. Soc.* **1992**, *114*, 6246. (b) Foucher, D. A.; Manners, I. *Macromol. Rapid Commun.* **1993**, *14*, 63. (c) Pannell, K. H.; Dementiev, V. V.; Li, H.; Cervantes-Lee, F.; Nguyen, M. T.; Diaz, A. F. *Organometallics* **1994**, *13*, 3644. (d) Gomez-Elipe, P.; Macdonald, P. M.; Manners, I. *Angew. Chem., Int. Ed. Engl.* **1997**, *36*, 762. (e) Manners, I. *Chem. Commun.* **1999**, *10*, 857.

(4) (a) Nelson, J.; Rengel, H.; Manners, I. *J. Am. Chem. Soc.* **1993**, *115*, 7035. (b) Nelson, J. M.; Nguyen, P.; Petersen, R.; Rengel, H.; Macdonald, P. M.; Lough, A. J.; Manners, I.; Raju Nandvale, P.; Greedan, J. E.; Barlow, S.; O'Hare, D. *Chem.−Eur. J.* **1997**, *3*, 573. For ROP of [2]ferrocenophanes with C−P and C−S bridges see: (c) Resendes, R.; Nelson, J. M.; Fischer, A.; Jäkle, F.; Bartole, A.; Lough, A. J.; Manners, I. *J. Am. Chem. Soc.* **2001**, *123*, 2116.

(5) For recent work on other strained metallocenophanes and related species see: (a) Braunschweig, H.; Buggisch, N.; Englert, U.; Homberger, M.; Kupfer, T.; Leusser, D.; Lutz, M.; Radacki, K. *J. Am. Chem. Soc.* **2007**, *129*, 4840. (b) Perrotin, P.; Shapiro, P. J.; Williams, M.; Twamley, B. *Organometallics* **2007**, *26*, 1823. (c) Tamm, M.; Kunst, A.; Bannenberg, T.; Randoll, S.; Jones, P. G. *Organometallics* **2007**, *26*, 417. (d) Elschenbroich, C.; Plackmeyer, J.; Nowotny, M.; Behrent, A.; Harms, K.; Pebler, J.; Burghaus, O. *Chem.−Eur. J.* **2005**, *11*, 7427. (e) Lund, C. L.; Schachner, J. A.; Quail, J. W.; Müller, J. *J. Am. Chem. Soc.* **2007**, *129*, 9313. (f) Vogel, U.; Lough, A. J.; Manners, I. *Angew. Chem., Int. Ed.* **2004**, *43*, 3321. (g) Mizuta, T.; Imamura, Y.; Miyoshi, K. *J. Am. Chem. Soc.* **2003**, *125*, 2068. (h) Chadha, P.; Dutton, J. L.; Sgro, M. J.; Ragogna, P. J. *Organometallics* **2007**, *26*, 6063.

(6) (a) Ni, Y.; Rulkens, R.; Manners, I. *J. Am. Chem. Soc.* **1996**, *118*, 4102. (b) Tanabe, M.; Vandermeulen, G. W. M.; Chan, W. Y.; Cyr, P. W.; Vanderark, L.; Rider, D. A. ; Manners, I. *Nat. Mater.* **2006**, *5*, 467. (c) Tanabe, M.; Manners, I. *J. Am. Chem. Soc.,* **2004**, *126*, 11434.

10.1021/om700941v CCC: $40.75
Publication on Web 03/13/2008

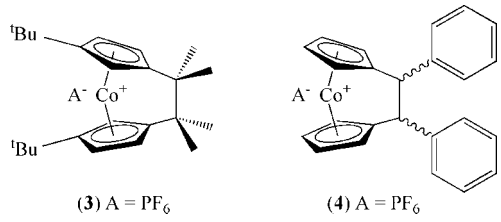

(**3**) A = PF_6 (**4**) A = PF_6

Figure 1. Cationic, hydrocarbon-bridged [2]cobaltoceniumphane salts **3** and **4**. Both species contain a Co(III) center with a d^6 valence electron configuration and are diamagnetic.

Most of the interesting functional properties of polyferrocenes are determined by the presence of iron centers. High molecular weight polymetallocenes with late transition metal centers, such as Co, in the main chain still remain virtually unexplored.[7,8] An important and interesting feature of polycobaltocenes is their stable, 18-electron polycationic structure. The charges along the polymer backbone should enhance the solubility in polar solvents, such as water, and hence lead to desirable, new materials. In contrast, polyferrocenes, which are uncharged in their 18-electron state unless functionalized in the side chain (e.g. by quaternized ammonium groups)[9] are typically soluble in solvents of limited polarity (e.g., benzene and toluene), whereas they are essentially insoluble in polar solvents such as methanol and water.[3e]

The amount of ring strain present for a ring-tilted metallocenophane is governed by the d electron configuration of the metal center.[2a,10] Theoretical studies suggest that metallocenophanes with less than two d electrons are essentially unstrained. Even in d^4 metallocenophanes, such as $WCl_2(\eta^5\text{-}C_5H_4)_2SiMe_2$, evidence for ring strain is not generally apparent.[2a,10] However, cationic, hydrocarbon-bridged [2]cobaltoceniumphane salts (with a d^6 configuration), which are isoelectronic to hydrocarbon-bridged [2]ferrocenophanes, would be expected to possess similar ring strain and propensity towards ROP to the latter. Only two hydrocarbon-bridged [2]cobaltoceniumphane salts have been reported in the literature (Figure 1): the first species with a $(CMe_2)_2$ bridge, **3**,[11] and the second with a $(CHPh)_2$ bridge, **4**,[12] both involving Co(III) centers.

Species **3** was prepared from the reaction of $CoBr_2$ with $(MgClC_5H_4)_2C_2Me_4 \cdot (THF)_x$, which was derived from the Mg-induced reductive dimerization of a *t*Bu-substituted 6,6-dimethylfulvene.[11] [2]Cobaltoceniumphane **4** was prepared from the treatment of $CoCl_2$ with $Ca(\eta^5\text{-}C_5H_4)_2(CHPh)_2 \cdot (THF)_2$, which was obtained via the Ca-mediated reductive dimerization of 6-phenylfulvene.[12] The unsymmetrical steric demand of the fulvene used in this synthesis determines the *meso* and *rac* distribution (30:70) of the product.[13] The low-valent metal-mediated reductive dimerization of appropriate fulvenes is versatile; however, its limitations are manifested in the substitution pattern in the 6-position of the fulvene (e.g., Me_2 in **3** and Ph in **4**), which is necessary to stabilize the intermediate radical anion sufficiently in order to dimerize.[14a,b] As a consequence, all metallocenophanes obtained via this route share a common design feature: a sterically demanding bridging moiety. This is assumed to facilitate the formation of the monomeric metallocenophane, while at the same time disfavoring ring-opening reactions. In order to synthesize cobaltocenophanes with reduced steric bulk in the bridge, other synthetic approaches have to be considered.[15]

In this article we present our results on the isolation and characterization of the first paramagnetic hydrocarbon-bridged [*n*]cobaltocenophanes ($n = 2, 3$) with reduced steric hindrance in the bridging moiety via the flytrap[2a] approach. The reduced steric demand of the bridging moiety in these monomers should lead to an increased propensity towards ROP. The metallocenophanes presented contain a Co(II) center with a d^7 valence electron configuration. Moreover, we report their oxidation to stable, cationic, and diamagnetic Co(III) species with a d^6 valence electron configuration.

Results and Discussion

(i) Synthesis and Characterization of Neutral 19-Electron [*n*]Cobaltocenophanes 5 and 6 ($n = 2, 3$). The neutral hydrocarbon-bridged [*n*]cobaltocenophanes **5** and **6** ($n = 2, 3$) were prepared by the reaction of $CoCl_2$ and the corresponding flytrap ligand $(LiC_5H_4)_2(CH_2)_n$ ($n = 2, 3$) in THF (Scheme 2). After vacuum sublimation **5** and **6** were obtained as black crystalline materials in very low yields of 9% and 8%, respectively. The identity of the paramagnetic, 19-electron species **5** and **6** was confirmed by elemental analysis, high-resolution mass spectrometry, single-crystal X-ray diffraction, and UV–vis spectrometry. All data obtained were consistent with the assigned structures.

We attribute the very low yields obtained to the small size of the substituents on the $(CH_2)_n$ backbone ($n = 2, 3$) and their modest influence on the conformational preference of the

(7) (a) Several reports of oligo- and polycobaltocenes have been made. For example: oligomethylene cobaltocenium cations as potential anion exchange materials: Ito, T.; Kenjo, T. *Bull. Chem. Soc. Jpn.* **1968**, *41*, 614. (b) Oligo- and poly[bis(oxycarbonylcyclopentadienyl)cobalt(III)(dicyclopentadienyltitanium(IV)) hexafluorophosphate] (characterized using IR techniques and thermal analysis: Carraher, C. E., Jr.; Sheats, J. E. *Makromol. Chem.* **1973**, *166*, 23. (c) Well-characterized oligomers with up to six repeat units of optically active cobaltocenium complexes where the metal centers are connected via π-conjugated [9]helicene units: Katz, T. J.; Sudhakar, A.; Teasley, M. F.; Gilbert, A. M.; Geiger, W. E.; Robben, M. P.; Wuensch, M.; Ward, M. D. *J. Am. Chem. Soc.* **1993**, *115*, 3182.

(8) Regarding electronic communication between metal centers in polymetallocenes, complexes with saturated single atom bridges can serve as a model. Studies on the electronic coupling in monocationic dimeric ferrocenes and cobaltocenes of the type $[\{M\text{-}(\eta^5\text{-}C_5Me_4)(\eta^5\text{-}C_5H_4)\}_2X]$ (M = Fe, Co, X = CMe_2, $SiMe_2$, $GeMe_2$) have shown that intervalence charge transfer proceeds predominantly via through-space mechanisms and that electronic coupling is much stronger in systems based on Co compared to systems based on Fe: Jones, S. C.; Barlow, S.; O'Hare, D. *Chem.—Eur. J.* **2005**, *11*, 4473. This work suggests that analogous polycobaltocenes should be very interesting to study.

(9) (a) Ginzburg, M.; Galloro, J.; Jäkle, F.; Power-Billard, K. N.; Yang, S.; Sokolov, I.; Lam, C. N. C.; Neumann, A. W.; Manners, I.; Ozin, G. A. *Langmuir* **2000**, *16*, 9609. (b) Ma, Y.; Hempenius, M. A.; Vancso, G. J. *J. Inorg. Organomet. Polym.* **2007**, *17*, 3. (c) Power-Billard, K. N.; Manners, I. *Macromolecules* **2000**, *33*, 26.

(10) Green, J. C. *Chem. Soc Rev.* **1998**, *27*, 263.

(11) Drewitt, M. J.; Barlow, S.; O'Hare, D.; Nelson, J. M.; Nguyen, P.; Manners, I. *J. Chem. Soc., Chem. Commun.* **1996**, 2153.

(12) Fox, S.; Dunne, J. P.; Tacke, M.; Schmitz, D.; Dronskowski, R. *Eur. J. Inorg. Chem.* **2002**, 3039.

(13) Kane, K. M.; Shapiro, P. J.; Vij, A.; Cubbon, R.; Rheingold, A. L. *Organometallics* **1997**, *16*, 4567.

(14) (a) Rieckhoff, M.; Pieper, U.; Stalke, D.; Edelmann, F. T. *Angew. Chem., Int. Ed. Engl.* **1993**, *32*, 1079. Rieckhoff, M.; Pieper, U.; Stalke, D.; Edelmann, F. T. *Angew. Chem.* **1993**, *105*, 1102. (b) Tacke, M.; Fox, S.; Cuffe, L.; Dunne, J. P.; Hartl, F.; Mahabiersing, T. *J. Mol. Struct.* **2001**, *559*, 331.

(15) A generally applicable method for the synthesis of *ansa*-sandwich complexes is the dimetalation of the parent sandwich complex. For representative examples see: (a) Bishop, J. J.; Davison, A.; Katcher, M. L.; Lichtenberg, D. W.; Merrill, R. E.; Smart, J. C. *J. Organomet. Chem.* **1971**, *27*, 241. (b) Elschenbroich, C.; Hurley, J.; Metz, B.; Massa, W.; Baum, G. *Organometallics* **1990**, *9*, 889. (c) Ogasa, M.; Rausch, M. D.; Rogers, R. D. *J. Organomet. Chem.* **1991**, *403*, 279. (d) Braunschweig, H.; Kupfer, T.; Radacki, K. *Angew. Chem.* **2007**, *119*, 1655. *Angew. Chem., Int. Ed.* **2007**, *46*, 1630. (e) Ref 2a. Unfortunately, efforts to react cobaltocene with ^{n}BuLi in the presence of multidentate coordinating tertiary amines such as tmeda (*N,N,N′,N′*- tetramethylethylenediamine) to produce an analogous 1,1′-dilithiated cobaltocene have been so far unsuccessful.

Scheme 2. Flytrap Synthesis of Neutral Hydrocarbon-Bridged Cobaltocenophanes 5 and 6 and Subsequent Oxidation to Produce Cationic Cobaltoceniumphane Salts 7–9

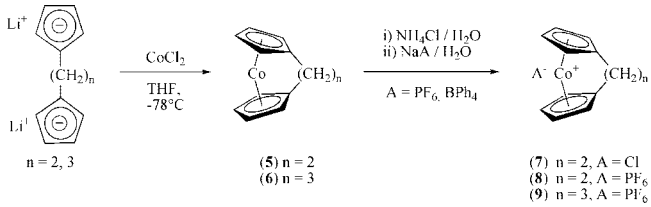

dianionic flytrap ligand precursor. After investigating the oxidative coupling of flytrap ligands of the type $(LiC_5H_4)_2(CH_2)_n$ ($n = 2-5$) using $CuCl_2$, Neuenschwander and co-workers argued that anti-isomer **A** (Figure 2) should be the favorable conformation for flytrap ligands where the substituents R are of limited steric demand. Increasing the steric bulk should promote steric repulsion between the substituents and hence lead to a stabilization of gauche-isomer **B** (Figure 2).[16] This is in accordance with the results for the preparation of **3** and **4**, which can be isolated in 21% and 43% yield, respectively, where the bridge substituents are substantially larger than those present in **5** and **6**.

A series of reference compounds to be used in order to discuss the structure and reactivity of neutral cobaltocenophanes **5** and **6** and cationic cobaltoceniumphane salts **7–9** are shown in Figure 3.

(ii) Discussion of the Single-Crystal X-Ray Structures of 5 and 6. Black crystalline blocks of **5** and **6** suitable for single-crystal X-ray analysis were obtained after vacuum sublimation at 40 and 55 °C, respectively. Crystals of **5** contain one and a half molecules per asymmetric unit and belong to the rhombohedral space group $P\bar{3}c1$, whereas crystals of **6** contain one molecule per asymmetric unit and belong to the noncentrosymmetric space group *Pn*. The discussion of the molecular structure of **5** is restricted to the molecule fully contained in the asymmetric unit (similar values within experimental error margins are obtained for the other half-molecule).[17]

The angles α, β, δ, and τ used in the discussion of the molecular structure of [*n*]metallocenophanes ($n = 2$, 3) are defined in Figure 4.

The basic molecular geometry about the cobalt center in both **5** and **6** is similar to that in **3** and **4**, i.e. the C_5H_4 moieties are bound in an η^5-fashion and the planes of these π-hydrocarbon rings subtend an angle α. The angle α reflects the distortion from coplanarity and can be used in conjunction with the β angles and $M-Cp_{centroid}$ bond distances to quantify the ring strain present. The distortion of the typical metallocene structure (as in cobaltocene $CoCp_2$ (**10**, α and β approximately 0°)[18e]) is large in **5** ($\alpha = 27.1(4)°$ and $\beta = 16.6(11)°/16.7(10)°$) and less pronounced in **6** ($\alpha = 12.0(11)°$ and $\beta = 4.0(2)°/3.5(14)°$) due to the shorter bridge in **5** compared to **6**. The distortion from coplanarity furthermore affects the δ angles, where a similar trend can be observed for progressively shorter bridges: $\delta =$ approximately 180° in **10**[18e] and $\delta = 171.0(5)°$ in **6** compared to $\delta = 158.0(16)°$ in **5**. As far as the variation of first row transition metal centers in otherwise identical ligand frameworks is concerned, the d electron configuration is the most influential parameter on the ring strain. Changing from Co(II) (d^7) in **5** ($\alpha = 27.1(4)°$, $\beta = 16.6(11)°/16.7(10)°$, and $\delta = 158.0(16)°$) to Fe(II) (d^6) in the corresponding [2]ferrocenophane **11** ($\alpha = 21.6(4)°$, $\beta = 20.1(3)°/12.7(3)°$, and $\delta = 164.1(3)°$)[4b] leads to a significant reduction in ring strain. A similar, yet less substantial effect can be observed comparing the [3]cobaltocenophane **6** ($\alpha = 12.0(11)°$, $\beta = 4.0(2)°/3.5(14)°$, and $\delta = 171.0(5)°$) and the corresponding [3]ferrocenophane **12** ($\alpha = 10.3°$, $\beta = 3.5°/4.1°$, and $\delta = 172.2(3)°$).[21] In a metallocene with a d^6 metal center, all molecular orbitals with bonding character are fully occupied. Additional valence electrons have to be accommodated in molecular orbitals with significant antibonding character. This reduction of the bond order leads to elongated $M-Cp_{carbon}$ distances and hence elongated $M-Cp_{centroid}$ distances. In ferrocene $FeCp_2$[18a,b] the average metal−C(Cp) distance is 2.04(3) Å compared to 1.997(5) Å in the isoelectronic and cationic $[CoCp_2][PF_6]$ **13**[18c,d] (the ionic interaction between the positively charged Co(III) center and the negatively charged Cp moieties in the latter leads to a decrease of the M−Cp distances compared to $FeCp_2$). In unbridged cobaltocene **10** a significant elongation of the average Co−C(Cp) distance to 2.096(8) Å[18e] can be observed. Due to the subtended angle α between the two ring moieties in *ansa*-metallocenes, it is more sensible to discuss $metal-Cp_{centroid}$ distances in these compounds because the individual $metal-Cp_{carbon}$ distances (C_α, C_β, and C_{ipso}) vary substantially. The $Co-Cp_{centroid}$ distance in **5** is 1.717(7)/1.714(7) Å, very similar to 1.719(2)/1.716(2) Å in **6**. For **5**, an angle τ can be characterized, which is specific to E−E bridged [2]metallocenophanes and describes the projected dihedral angle between the axis $Cp_{centroid}-M-Cp'_{centroid}$ and the E−E vector. In [2]cobaltocenophane **5**, this angle measures 21.9(15)° compared to 18.4(1)° in the corresponding [2]ferrocenophane **11**.

(iii) Synthesis and Characterization of Cationic [*n*]Cobaltoceniumphanes 7 and 8 (*n* = 2) and 9 (*n* = 3). The cationic [2]cobaltoceniumphane salt **7** was obtained as a yellow to orange solid in high yield (80%) after the oxidation of [2]cobaltocenophane **5** in an aqueous solution of NH_4Cl in the presence of atmospheric oxygen and a subsequent extraction with CH_2Cl_2. The salt **8** was prepared in a similar fashion: oxidation of **5** was followed by precipitation of **8** using a saturated solution of $NaPF_6$. The [3]cobaltoceniumphane salt **9** was prepared from **6** following an analogous synthetic protocol. The identity of compounds **8** and **9** was confirmed by ^1H and $^{13}C\{^1H\}$ NMR spectroscopy, HRMS, and elemental analysis. All the analytical data obtained were consistent with the assigned structures. The salt **7** could be prepared in only ca. 97% purity as observed by ^1H NMR and was furthermore characterized using $^{13}C\{^1H\}$ spectroscopy and HRMS.

For the diamagnetic d^6 [*n*]cobaltocenophane ($n = 2$, 3) cations in **7–9**, ^1H and $^{13}C\{^1H\}$ NMR spectra were recorded at ambient temperatures and are discussed using [2]cobaltoceniumphane **8** and [3]cobaltoceniumphane **9** as examples. In the ^1H NMR spectra of **8** and **9**, signals characteristic for a time-averaged C_{2v} symmetric metallocenophane were obtained. In the case of **8**, two distinguishable ^1H NMR pseudotriplets for H_α and H_β

(16) You, S.; Gubler, M.; Neuenschwander, M. *Helv. Chim. Acta* **1994**, *77*, 1346.

(17) Values for standard uncertainties involving Cp centroids (e.g., δ angles) were estimated by using the same standard uncertainty as for the corresponding Cp carbon atoms.

(18) (a) Dunitz, J. D.; Orgel, L. E.; Rich, A. *Acta Crystallogr.* **1956**, *9*, 373. (b) Seiler, P.; Dunitz, J. D. *Acta Crystallogr.* **1982**, *6*, 1741. (c) Braga, D.; Scaccianoce, L.; Grepioni, F.; Draper, S. M. *Organometallics* **1996**, *15*, 4675. (d) Grepioni, F.; Cojazzi, G.; Draper, S. M.; Scully, N.; Braga, D. *Organometallics* **1998**, *17*, 296. (e) Bünder, W.; Weiss, E. *J. Organomet. Chem.* **1975**, *92*, 65.

(19) Rosenblum, M.; Bannerjee, A. K.; Danieli, N.; Fish, R. W.; Schlatter, V. *J. Am. Chem. Soc.* **1963**, *85*, 316.

(20) Lentzner, H. L.; Watts, W. E. *Tetrahedron* **1971**, *27*, 4343.

(21) Kadkin, O.; Näther, C.; Friedrichsen, W. J. *J. Organomet. Chem.* **2002**, *694*, 161.

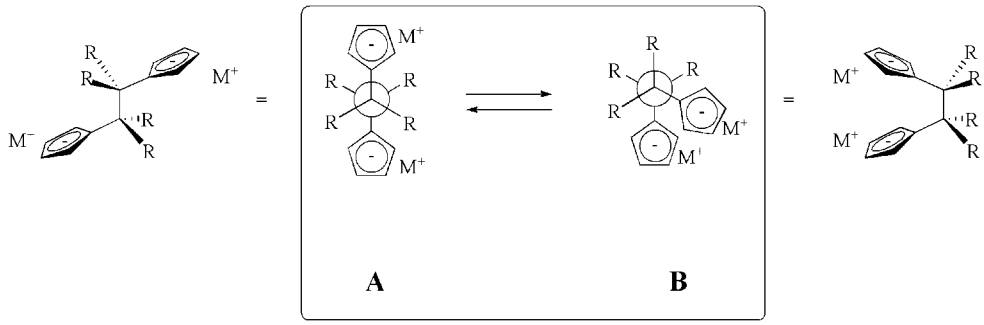

Figure 2. Schematic depiction of anti-isomers **A** and gauche-isomer **B** in flytrap ligand $[M^+]_2[(C_5H_4)_2(CH_2)_2]$, viewed along the carbon−carbon backbone. Isomer **A** with (C_5H_4) moieties in anti position should promote formation of linear and cyclic oligomers. The formation of monomeric metallocenophanes should be facilitated in the case of **B** with (C_5H_4) moieties in the *gauche* position.

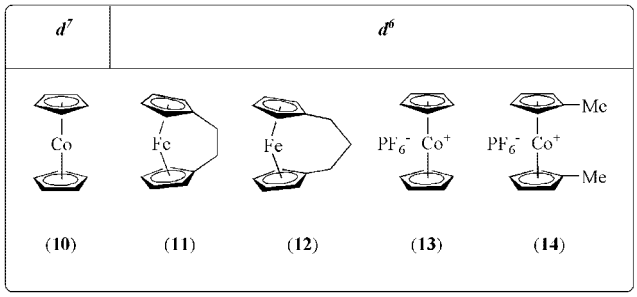

Figure 3. Reference compounds **10–14**.

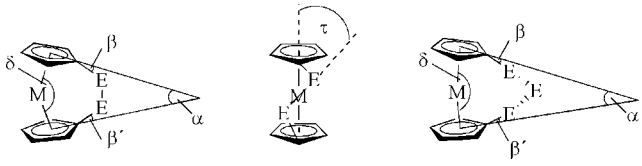

Figure 4. Geometric parameters α, β, δ, and τ in [2]- and [3]metallocenophanes with an E_n ($n = 2, 3$) bridge.

protons in the aromatic region at 6.37 and 5.35 ppm and a ^{1}H NMR singlet for the bridge protons at 3.32 ppm were observed. In the $^{13}C\{^1H\}$ NMR spectrum of **8**, four characteristic signals in accordance with time-averaged C_{2v} symmetry can be observed. For the bridging carbon atoms resonances appear at 33.7 ppm, and the C_α and C_β atoms resonate at 84.8 and 86.3 ppm. The most characteristic feature of strained hydrocarbon-bridged metallocenophanes is a downfield shifted resonance for C_{ipso}, which is detected in the case of **8** at 110.8 ppm.

Comparable features can be observed for [3]cobaltoceniumphane **9**: ^{1}H NMR pseudotriplets for H_α and H_β protons are apparent at 5.48 and 5.38 ppm with the difference in frequency between the resonances being less pronounced when compared to **8** and [2]ferrocenophane **11**. For the bridging moiety, two distinct signals for [3]cobaltoceniumphane **9** in a 2:1 ratio were observed at 1.85 and 1.98 ppm (the peak at 1.85 as a triplet, the peak at 1.98 as a multiplet). Furthermore, in the $^{13}C\{^1H\}$ NMR spectrum of **9**, two signals at 12.6 and 13.2 ppm were observed for the bridge. In case of the [3]cobaltoceniumphane **9** the most characteristic spectroscopic feature of the hydrocarbon-bridged metallocenophanes, the pronounced shift for the $^{13}C\{^1H\}$ NMR signal of the C_{ipso} atoms of the C_5H_4 rings, is not apparent. A signal for the C_{ipso} atom in **9** is detected at 103.7 ppm (compared to 104.6 ppm for the C_{ipso} atom in **14**[22b]). This confirms that the degree of separation between the H_α and H_β C_5H_4 protons, and the magnitude of the downfield shift is a function of the tilt angle α. For ferrocenophanes **11**[4,20] and **12**,[19] ^{1}H and $^{13}C\{^1H\}$ NMR data have been reported previously and are in accordance with the structure assigned from X-ray analysis.[4,21] Analogously to [*n*]cobaltoceniumphanes **8** ($n = 2$) and **9** ($n = 3$), two ^{1}H NMR pseudotriplets for the Cp ring protons are present at 4.6 and 3.9 ppm and a ^{1}H NMR singlet for the protons of the ethylene bridge is observed at 2.6 ppm for [2]ferrocenophane **11**. In addition, a characteristic downfield shift for the $^{13}C\{^1H\}$ NMR C_{ipso} resonance is detectable due to the ring strain present. The C_{ipso} signal for **11** in C_6D_6 is found at 91.2 ppm, compared to 68.8 and 72.9 ppm for C_α and C_β ring atoms.

(iv) Discussion of the Single-Crystal X-Ray Structural Analysis of 7. Blocks of light orange crystals of **7** suitable for single-crystal X-ray analysis were obtained after diffusing hexanes into a saturated solution of **7** in CH_2Cl_2. Crystals of **7** contain in addition to the target compound one molecule of H_2O per asymmetric unit and belong to the monoclinic space group $P2_1/c$. The molecular structure of **7** is related to the molecular structure of **5**, where a metallocenophane-type geometry (C_2) is adopted with significant deviation of the two C_5H_4 ring moieties from coplanarity as a result of the introduced C_2H_4 bridge. However, as a result of the d electron configuration, marked differences in between **7** (Co(III), d^6) and **5** (Co(II), d^7) can be observed regarding the degree of distortion (**5**: α = 27.1(4)°, β = 16.6(11)°/16.7(10)°, τ = 22.0(6)°, $M-Cp_{centroid}$ = 1.717(7)/1.714(7) Å; **7**: α = 21.4(2)°, β = 12.6(3)°/12.3(3)°, τ = 13.1(4)°, $M-Cp_{centroid}$ = 1.619(3)/1.615(3) Å) imposed by the otherwise identical ligand framework. In metallocenes with a d^6 electron configuration, all bonding orbitals are fully occupied, which leads to a bond order maximum. The assimilation of a further electron leads to a bond order decrease and a subsequent elongation of the M−Cp bond lengths. This effect is amplified by increased ionic interactions between the negatively charged C_5H_4 rings and an additional positive charge at the Co(III) metal center in **7** compared to that in **5**. The X-ray analysis of the corresponding isoelectronic C_2H_4-bridged [2]ferrocenophane **11** reveals nearly identical metric parameters to **7** (Table 1), which corroborates the assertion that in short-bridged metallocenophanes with late transition metals from the same row, the ring strain is a function of the d electron configuration.

(v) UV–Vis Spectroscopic Studies and Electronic Structures of 5, 6, 8, 9, and 14. In order to further probe the electronic structure of the neutral and cationic hydrocarbon-bridged cobaltocenophanes, solution UV–vis spectra in the range from 200 to 800 nm were recorded for compounds **5**, **6**, **8**, and **9** and the reference compound $[Co(\eta^5\text{-}C_5H_4Me)_2][PF_6]$ (**14**) (Figures 8 and 9). The visual appearance of the neutral, paramagnetic, 19-electron compounds **5** and **6** in solution is markedly different from the cationic, diamagnetic compounds **8** and **9**. For **5** and **6**, pale red and orange solutions respectively,

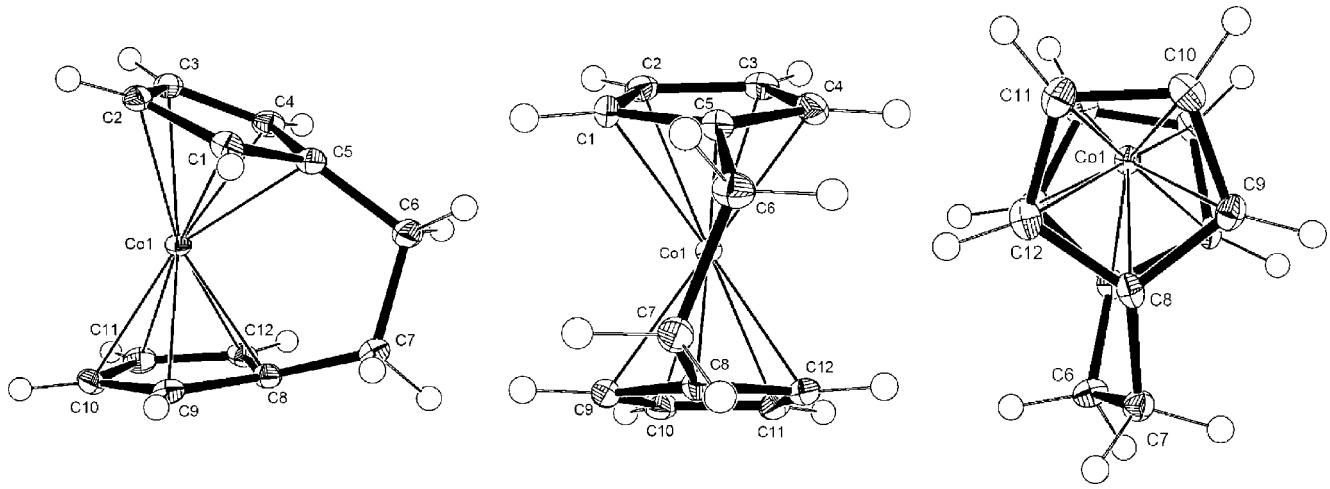

Figure 5. Three alternative views of the molecular structure of [2]cobaltocenophane **5** with thermal ellipsoids at the 50% probability level (hydrogen atoms have not been labeled for clarity). Selected bond lengths (Å) and angles (deg): Co1−C1 = 2.084(7), Co1−C2 = 2.131(6), Co1−C3 = 2.144(7), Co1−C4 = 2.079(7), Co1−C5 = 2.073(7), Co1−C8 = 2.076(7), Co1−C9 = 2.080(7), Co1−C10 = 2.145(7), Co1−C11 = 2.143(7), Co1−C12 = 2.068(7), C1−C2 = 1.433(10), C2−C3 = 1.424(9), C3−C4 = 1.428(10), C4−C5 = 1.429(9), C1−C5 = 1.437(9), C5−C6 = 1.512(9), C6−C7 = 1.554(9), C7−C8 = 1.514(9), C1−C5−C4 = 106.1(6), C5−C6−C7 = 111.9(6), C12−C8−C9 = 116.1(6).

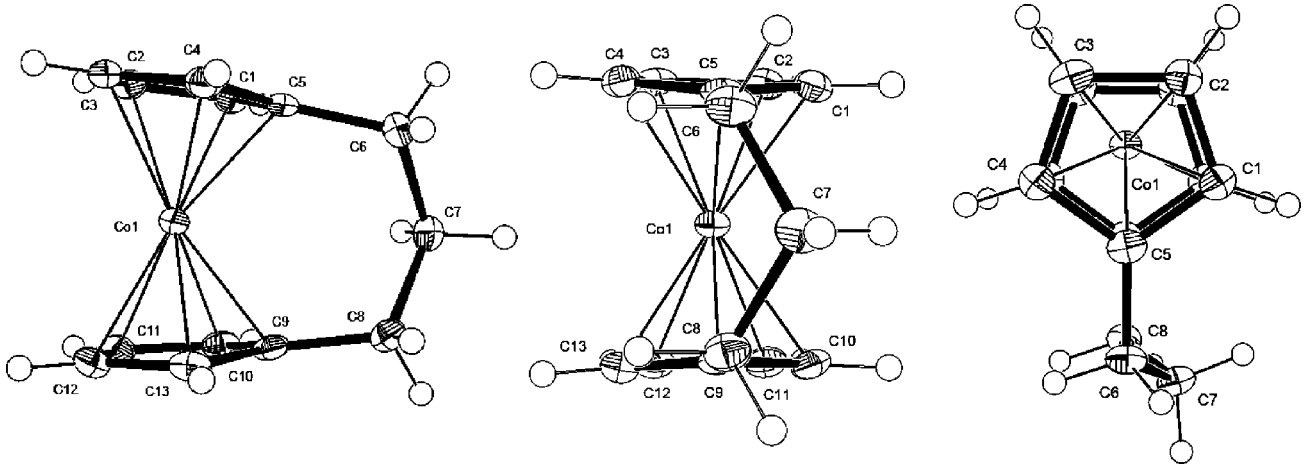

Figure 6. Three alternative views of the molecular structure of [3]cobaltocenophane **6** with thermal ellipsoids at the 50% probability level (hydrogen atoms have not been labeled for clarity). Selected bond lengths (Å) and angles (deg): Co1−C1 = 2.114(2), Co1−C2 = 2.115(3), Co1−C3 = 2.111(3), Co1−C4 = 2.1218(19), Co1−C5 = 2.0484(19), Co1−C9 = 2.0486(18), Co1−C10 = 2.113(2), Co1−C11 = 2.115(2), Co1−C12 = 2.111(2), Co1−C13 = 2.120(2), C1−C2 = 1.407(4), C2−C3 = 1.428(3), C3−C4 = 1.407(4), C4−C5 = 1.437(3), C5−C6 = 1.510(3), C6−C7 = 1.539(3), C1−C2−C3 = 108.5(2), C1−C5−C4 = 107.68(16), C5−C6−C7 = 115.31(17), C6−C7−C8 = 114.72(17).

were obtained in hexane, whereas **8**, **9**, and **14** exhibit a yellow color as methanol solutions. Solution UV–vis spectra for the paramagnetic, 19-electron [2]cobaltocenophane **5** and [3]cobaltocenophane **6** in hexanes are shown in Figure 8. Solution UV–vis spectra for the diamagnetic, 18-electron [2]cobaltoceniumphane salt **8** and [3]cobaltoceniumphane salt **9** in methanol are shown in Figure 9.

An assignment of the three UV–vis bands for cobaltocene and nickelocene in the solid state has been undertaken by Ammeter and co-workers.[26] Three characteristic absorbances can also be observed for **5** at 264 nm (ϵ = 6465 L mol^{-1} cm^{-1}), 326 nm (ϵ = 3448 L mol^{-1} cm^{-1}), and 486 nm (ϵ = 554 L mol^{-1} cm^{-1}). A red shift of the lowest energy absorbance λ_{max} in [2]cobaltocenophane **5** relative to that of [3]cobaltocenophane **6** is apparent, where this band has an unresolved shoulder around 380 nm. The observed red shift and intensity increase detected for [2]cobaltocenophane **5** relative to [3]cobaltocenophane **6** correlates with the increased tilt angle and is analogous to that detected in [1]ferrocenophanes.[27] Only two resolved absorbances can be observed for **6** at 266 nm (ϵ = 9739 L mol^{-1} cm^{-1}) and 322 nm (ϵ = 4932 L mol^{-1} cm^{-1}).

The UV–vis spectra for **13** and **14** in methanolic solution have been recorded by El Murr and show three characteristic absorbances in the region between 240 and 450 nm.[22a] For d^6-metallocenes, high-energy absorptions (ca. 200–270 nm, band IV) can be generally assigned to ligand-to-metal charge transfer (LMCT) transitions, whereas the absorptions at longer wavelengths (around 320 nm, band III, and 400 nm, band II) are predominantly Laporte forbidden d−d transitions between filled e′ and a_1′ HOMO and empty e″ LUMO orbitals.[23a,b] The introduction of a short bridge to a d^6 metallocene lowers the symmetry from D_{5h} (for the assignment of molecular orbitals in unbridged $FeCp_2$ D_{5h} symmetry is assumed)[18a,b] to a time-averaged C_{2v} symmetry in solution. Thereby a characteristic influence on the UV–vis spectra can be observed: lowering the symmetry induces a splitting of the filled, nonbonding e_{2g}

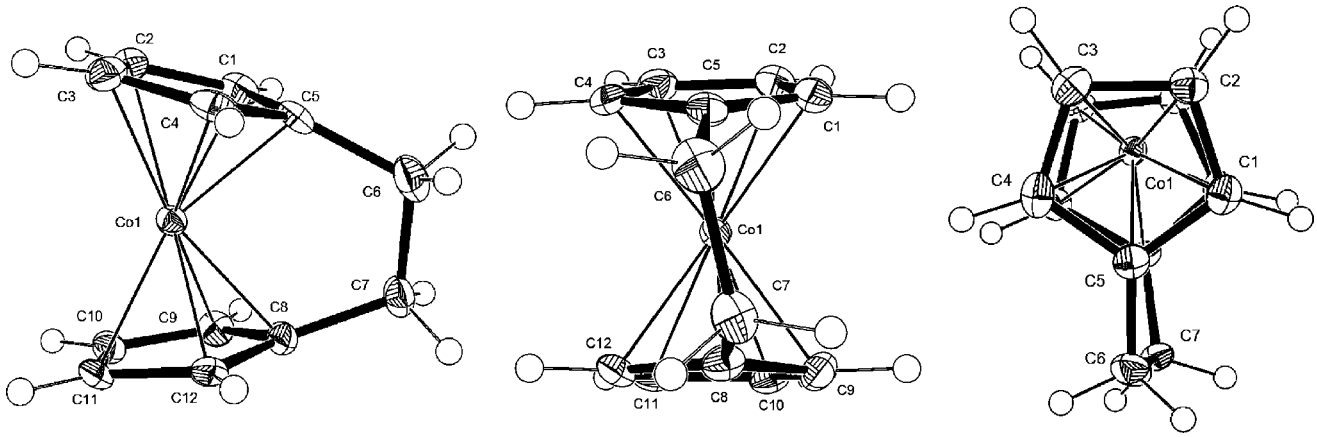

Figure 7. Three alternative views of the molecular structure of the cation in [2]cobaltoceniumphane salt **[7]**·H_2O with thermal ellipsoids at the 50% probability level. Hydrogen atoms have not been labeled and the counterion, as well as one molecule of H_2O, have been omitted for clarity. Selected bond lengths (Å) and angles (deg): Co1−C1 = 2.015(4), Co1−C2 = 2.058(3), Co1−C3 = 2.051(3), Co1−C4 = 2.015(3), Co1−C5= 1.971(3), Co1−C8 = 1.973(3), Co1−C9 = 2.023(3), Co1−C10 = 2.064(3), Co1−C11 = 2.058(3), Co1−C12 = 2.012(3), C1−C2 = 1.427(5), C2−C3 = 1.432(5), C3−C4 = 1.424(5), C4−C5 = 1.438(5), C5−C6 = 1.535(5), C6−C7 = 1.534(4), C7−C8 = 1.512(4), C1−*C2*−C3 = 107.6(3), C1−C5−C4 = 107.2(3), C5−C6−C7 = 111.8(3), C6−C7−C8 = 112.7 (3).

Table 1. Structural Parameters for Neutral and Cationic [*n*]Cobaltocenophanes and [*n*]Ferrocenophanes (*n* = 2, 3)

compound	α [deg]	*β* [deg]	*δ* [deg]	M−$Cp_{centroid}$ [Å]	ref
3[a]	24.8	9.2	162.1	1.630(2)	11
4	22.9	12.1/12.3	163.1	1.617	12
5	27.1(4)	16.6(11)/16.7(10)	158.0(16)	1.717(7)/1.714(7)	this work
6	12.0(11)	4.0(2)/3.5(14)	171.0(5)	1.719(2)/1.716(2)	this work
7	21.4(2)	12.6(3)/12.3(3)	164.0(1)	1.619(3)/1.615(3)	this work
11[b]	21.6(4)	20.1(3)/12.7(3)	164.1(3)	1.629(6)	4b
12	10.3	3.5/4.1	172.2	1.637(2)	21

[a] One of the *t*Bu groups is disordered. [b] The C_2 bridge is disordered over two sites with occupancies of 0.60 and 0.40, respectively.

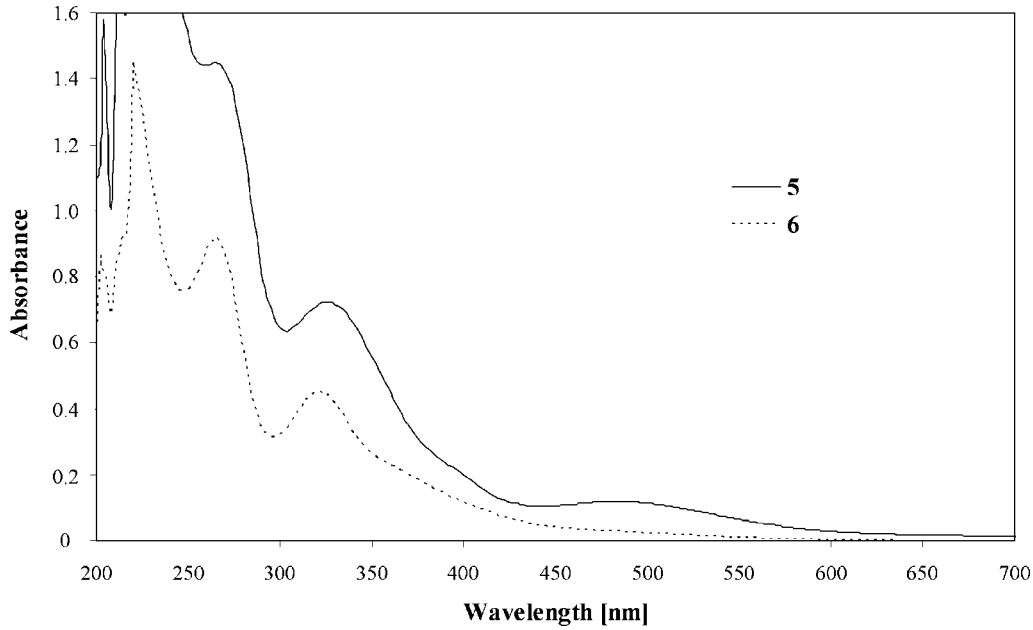

Figure 8. UV–vis spectrum of **5** (top) and **6** (bottom) in hexane (0.00228 mM for **5** and 0.946 mM for **6**).

orbitals, which leads to a resolution of two closely spaced bands IIa and IIb. The λ_{max} of the lowest-energy band IIa undergoes a pronounced bathochromic shift in [1]ferrocenophanes as a function of the tilt angle α, which has been rationalized by employing EHMO and DFT calculations.[24] Furthermore, the intensity of the low-energy d−d transitions increases as a function of α. Forcing the two Cp units out of their coplanar arrangement leads to a relaxation of the Laporte selection rules (i.e. larger extinction coefficients) and a possibly increased contribution of the Cp ligand to the LUMO orbital character.[10,24,25] In accordance with this, three characteristic features can be extracted from the comparison of the solution UV–vis spectra for compounds **8**, **9**, and **14**. For the unbridged cobaltocenium cation **14**, a distinctive shoulder around 316 nm can be observed. Upon the introduction of relatively modest distortion as in the [3]cobaltoceniumphane cation in **9**, the shoulder is less explicit, and it nearly disappears for the more highly distorted ethane-bridged **8**, while simultaneously, a bathochromic shift of λ_{max}

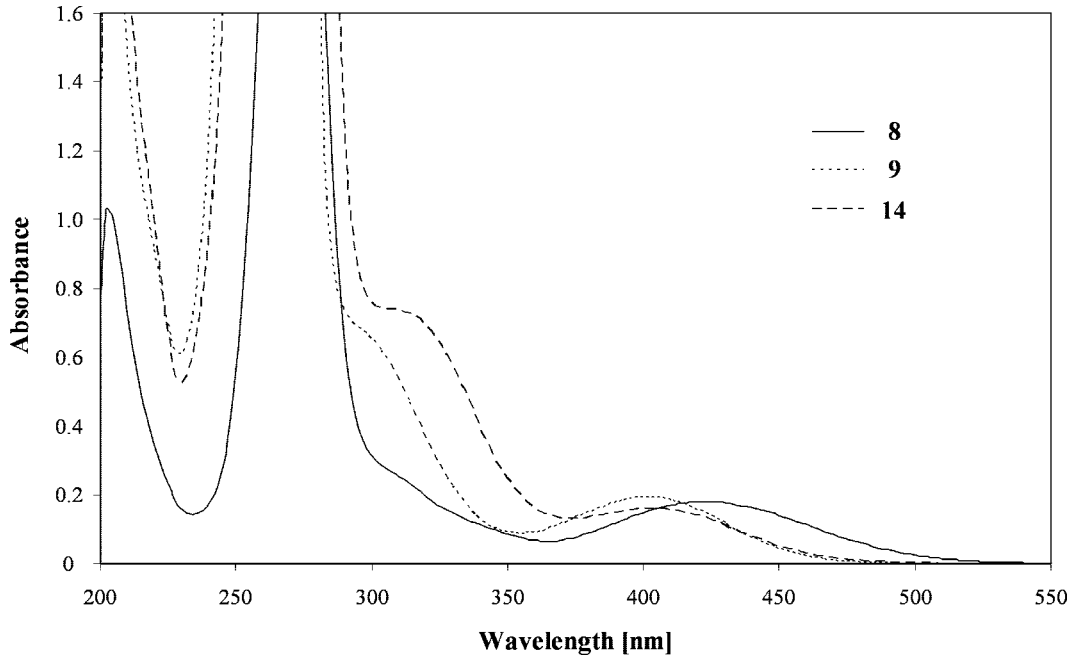

Figure 9. UV–vis spectrum of **8**, **9**, and **14** in methanol (0.173 mM for **8**, 0.517 mM for **9**, and 0.543 mM for **14**).

for the lowest-energy absorbance occurs from 402 nm in **9** to 422 nm in **8**. An increase of the molar absorption coefficients can be observed as a function of α, e.g., regarding λ_{max} of band IIa ($\epsilon = 293$ L mol^{-1} cm^{-1} for **14** (402 nm), $\epsilon = 362$ L mol^{-1} cm^{-1} for **9** (402 nm), and $\epsilon = 1009$ L mol^{-1} cm^{-1} for **8** (422 nm)).

(vi) Cyclic Voltammetric Analysis of Hydrocarbon-Bridged Cationic [2]Cobaltoceniumphane 8, [3]Cobaltoceniumphane 9 and Reference Compound [Co(η^5-$C_5H_4Me)_2$]-[PF_6] (14). The [*n*]cobaltoceniumphane cation in **8** and **9** was studied in order to determine whether the transmission of electronic effects or the electrochemical reversibility of the cobaltocenium/cobaltocene couple would be significantly affected as a consequence of the introduction of progressively shorter hydrocarbon bridges. The electrochemical behavior of **14** has been studied by El Murr and is included here as an unbridged and hence unstrained reference compound.[22a] Figure 10 shows the cyclic voltammograms of compounds **8**, **9**, and **14** obtained from 1.0×10^{-3} mol L^{-1} solutions in methylene chloride and 0.1 mol L^{-1} in [N^{n}Bu$_4$][PF_6] as the supporting electrolyte. The voltammograms were obtained at room temperature with a scan rate of 200 mV s^{-1} and are referenced to the [Fe(η^5-$C_5Me_5)_2$]/[Fe(η^5-$C_5Me_5)_2$]$^+$ couple at −0.08 V. Under the conditions applied during our studies, **8**, **9**, and **14** exhibit a reduction from cationic Co(III) to neutral Co(II) (Scheme 3).

Gassman has reported that the methylation of the Cp rings in substituted ferrocenes reduces the oxidation potential by 55 mV per methyl group.[28a] Similarly, it has been demonstrated for silicon-bridged [1]ferrocenophanes that the oxidation potential is a function of the degree of methylation on the Cp rings (ca. 50 mV reduction per methyl group).[28b] In the case of cationic 18-electron [*n*]cobaltoceniumphane salts **8** ($n = 2$) and **9** ($n = 3$), the reduction potential appears to depend on ring tilt. Thus, a reduction wave was found for the unstrained reference compound [Co(η^5-$C_5H_4Me)_2$][PF_6], **14**, at −1.00 V under the conditions applied (Figure 10). In comparison, for the cation in the propane-bridged [3]cobaltoceniumphane salt **9** a shift of the half-wave reduction potential to a more negative value at −1.05 V was observed. The distortion induced by the propane linker is not dramatic, and therefore this shift may also arise from the increased electron-donating nature of the ligand due to an additional CH_2 unit in the bridge. However, the introduction of a significantly shorter *ansa*-bridge in the cation in **8** compared to that in **9** shifts the value of the half-wave reduction potential to −0.91 V. In addition to the shorter and hence less electron-donating *ansa*-bridge compared to that in **9**, the substantial distortion from metallocene-type geometry has to be considered. In 18-electron metallocene-type compounds, all the degenerate HOMO orbitals are fully occupied and additional electrons need to be accommodated upon reduction in LUMO orbitals with significant antibonding character. The EHMO comparison for the frontier orbitals in [1]ferrocenophanes revealed a decrease of the HOMO–LUMO gap as a function of an increasing tilt angle.[24] When comparing

(22) (a) El Murr, N. *J. Organomet. Chem.* **1976**, *112*, 189. (b) Materikova, R. B.; Babin, V. N.; Lyatifov, I. R.; Salimov, R. M.; Fedin, E. I.; Petrovskii, P. V. *J. Organomet. Chem.* **1981**, *219*, 259.

(23) (a) Sohn, Y. S.; Hendrickson, D. N.; Gray, H. B. *J. Am. Chem. Soc.* **1971**, *93*, 3603. (b) Yamaguchi, Y.; Ding, W.; Sanderson, C. T.; Borden, M. L.; Morgan, M. J.; Kutal, C. *Coord. Chem. Rev.* **2007**, *251*, 515.

(24) Rulkens, R.; Gates, D. P.; Balaishis, D.; Pudelski, J. K.; McIntosh, D. F.; Lough, A. J.; Manners, I. *J. Am. Chem. Soc.* **1997**, *119*, 10976.

(25) Barlow, S.; Drewitt, M. J.; Dijkstra, T.; Green, J. C.; O'Hare, D.; Whittingham, C.; Wynn, H. H.; Gates, D. P.; Manners, I.; Nelson, J. M.; Pudelski, J. K. *Organometallics* **1998**, *17*, 2113.

(26) Ammeter, J. H.; Swalen, J. D. *J. Chem. Phys.* **1972**, *57*, 678.

(27) (a) It is noteworthy that the introduction of short bridges into metallocene-type systems does not necessarily lead to a bathochromic shift of λ_{max} for the lowest-energy absorbance. If short bridges containing silicon and germanium moieties are introduced in heteroleptic (η^7-C_7H_6)Cr(η^5-C_5H_5), bathochromic shifts can be observed: Braunschweig, H.; Kupfer, T.; Lutz, M.; Radacki, K. *J. Am. Chem. Soc.* **2007**, *129*, 8893. In contrast to this, hypsochromic shifts of the lowest-energy absorbance have been detected upon the introduction of $SiMe_2$ bridges in the titanium congener (η^7-C_7H_6)Ti(η^5-C_5H_5): Tamm, M.; Kunst, A.; Bannenberg, T.; Herdtweck, E.; Sirsch, P.; Elsevier, C. L.; Ernsting, J. M. *Angew. Chem.* **2004**, *116*, 5646; *Angew. Chem., Int. Ed.* **2004**, *43*, 5530.

(28) (a) Gassman, P. G.; Macomber, D. W.; Hershberger, J. W. *Organometallics* **1983**, *2*, 1470. (b) Pudelski, J. K.; Foucher, D. A.; Honeyman, C. H. Lough, A. J.; Manners, I.; Barlow, S.; O'Hare, D. *Organometallics* **1995**, *14*, 2470.

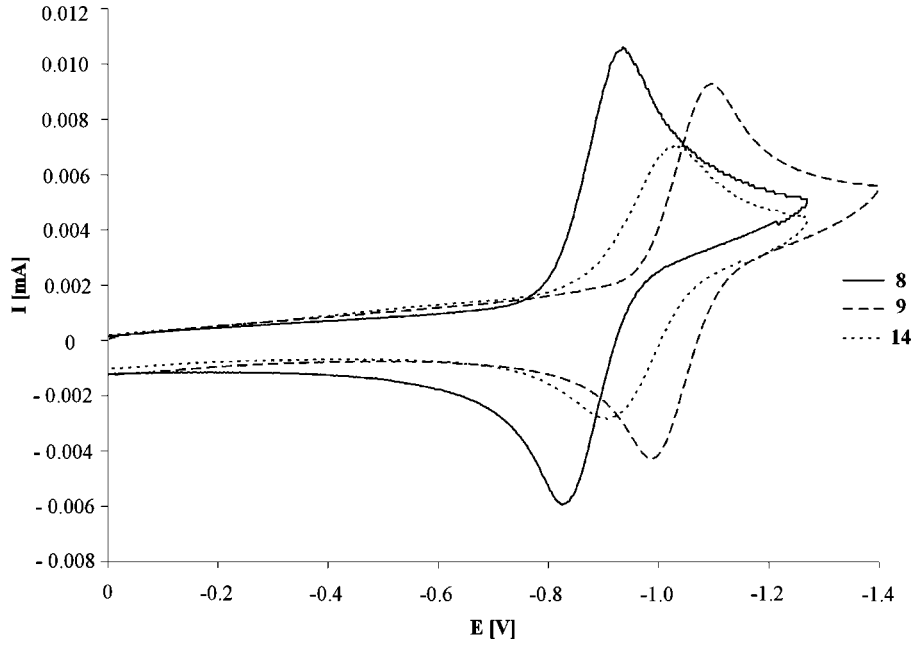

Figure 10. Cyclic voltammograms of CH_2Cl_2 solutions of **8**, **9**, and **14** obtained at room temperature with a scan rate of 200 mV s^{-1} and referenced to the $[Fe(C_5Me_5)_2]/[Fe(C_5Me_5)_2]^+$ couple at −0.08 V.

Scheme 3. Electrochemical Reduction of Cationic [*n*]Cobaltoceniumphanes 8 (*n* = 2) and 9 (*n* = 3)

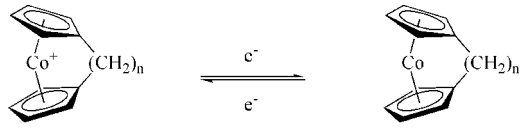

(**8**) n = 2
(**9**) n = 3

(**5**) n = 2
(**6**) n = 3

[2]cobaltoceniumphane **8** and [3]cobaltoceniumphane **9**, the distinct shift to less negative reduction potential with increased tilt indicates lowering of the energetic level of the LUMO orbital relative to the HOMO orbital.

Summary

Synthetic routes to neutral, 19-electron, paramagnetic hydrocarbon-bridged [*n*]cobaltocenophanes **5** and **6** (*n* = 2, 3) with a d^7 valence electron configuration and their cationic, 18-electron, diamagnetic analogues in the salts **7**–**9** with a d^6 valence electron configuration have been developed. The increasingly shorter bridges lead to interesting structural changes, such as an increase in ring tilt. The presence of an electron in an antibonding orbital leads to longer and weakened Co−Cp bonds in **5** relative to the cation in **7**, which results in a larger ring tilt (α = 27.1(4)° vs 21.4(2)°). Electrochemical investigations revealed reversible one-electron reductions of the cobaltoceniumphane cations in **8** and **9**, whereby the value of the half-wave potential is a function of the ring tilt. Studies to investigate the potential of all of the cobaltocenophanes presented as monomers for ROP are in progress, and the results will be reported in future publications.

Experimental Section

General Comments. All reactions were carried out under atmospheres of either dry dinitrogen or dry argon using standard Schlenk line techniques or an MBraun glove box MB150B-G. Dry N_2-saturated THF and hexane were collected from a Grubbs-type solvent system using filtration through an alumina column impregnated with deoxygenated catalysts. NMR spectra were recorded on a JEOL Delta GX 400 (^{1}H: 400 MHz, ^{13}C: 100 MHz), an Eclipse 400 (^{1}H: 400 MHz, ^{13}C: 100 MHz), or an Eclipse 300 (^{1}H: 300 MHz, ^{13}C: 75.4 MHz) spectrometer at ambient temperatures, with all resonances referenced to residual NMR solvent resonances. UV–vis data were obtained on a Lambda 35 spectrometer employing standard quartz cells (0.01 m) from 200 to 800 nm with a scan rate of 2 nm s^{-1}. Electrochemical studies were carried out using an EG&G model 273A potentiostat linked to a computer using EG&G model 270 Research Electrochemistry software in conjunction with a three-electrode cell. The working electrode was a platinum disk (1.6 mm diameter), and the auxiliary electrode a platinum wire. The reference was an aqueous saturated calomel electrode separated from the test solution by a fine porosity frit and an agar bridge saturated with KCl. Solutions were 1.0×10^{-3} mol L^{-1} in the test compound and 0.1 mol L^{-1} in $[N^nBu_4][PF_6]$ as the supporting electrolyte; the solvent used was CH_2Cl_2. Under these conditions, $E^{\circ\prime}$ for the one-electron oxidation of $[Fe(\eta^5\text{-}C_5Me_5)_2]$ added to the test solutions as internal calibrant was −0.08 V. Unless specified, all $(E_p)_{red}$, $(E_p)_{ox}$, and $E^{\circ\prime}$ values are at a scan rate v of 200 mV s^{-1}.[29] Crystallographic experimental data are presented in Table 2. Single crystals of compounds **5** and **6** were coated in perfluoropolyether oil and mounted on glass fibers. X-ray diffraction data were measured on Bruker-AXS SMART 1k (**5**) and Bruker-AXS SMART-Apex (**6**) diffractometers using Mo Kα radiation (λ = 0.71073 Å).[30] Intensities were integrated[31] from several series of exposures, each exposure covering 0.3° in ω. Crystallographic data for compound **7** were collected at the EPSRC National Crystallography Service using a Bruker-AXS FR591 rotating anode diffractometer with Mo Kα radiation (λ = 0.71073 Å).[32] Intensities were integrated[33] from several series of exposures, each exposure covering a narrow angle in ω or φ. For all three compounds,

(29) Kissinger, P. T.; Heinemann, W. R. *J. Chem. Educ.* **1983**, *60*, 702.
(30) *SMART* diffractometer control software version 5; Bruker AXS: Madison, WI, 1997−2002.
(31) *SAINT* integration software version 7; Bruker AXS: Madison, WI, 1997–2003.
(32) Hooft, R. W. W. *COLLECT* data collection software; Nonius B. V.: Delft, The Netherlands, 1998.
(33) Otwiowski, Z.; Minor, W. Processing of X-ray diffraction data collected in oscillation mode. *Macromol. Crystallogr., Part A* **1997**, *276*, 307.

Table 2. Crystallographic Data for Compounds 5–7

	5	6	7
cryst syst	trigonal	monoclinic	monoclinic
a/Å	24.747(4)	6.278(2)	7.1957(2)
b/Å	24.747(4)	7.280(3)	10.2972(4)
c/Å	7.4616(15)	10.834(4)	14.7117(6)
α/deg	90	90	90
β/deg	90	101.286(6)	92.524(2)
γ/deg	120	90	90
V/Å^3	3957.4(11)	485.6(3)	1089.01(7)
T/K	100	173	120
space group	$P\bar{3}c1$	*Pn*	$P2_1/c$
Z	18	2	4
no. of reflns (measd/unique/obsd)[a]	27 394/3036/2406	4946/2123/2011	10 805/2505/2147
R_{int}	5.0%	2.4%	4.8%
R_1 (obsd reflns)	6.8%	2.0%	4.3%
wR_2 (all reflns)	22.8%	4.7%	15.0%

[a] Observation criterion $I > 2\sigma(I)$.

absorption corrections were applied, based on multiple and symmetry-equivalent measurements.[34] The structures were solved by direct methods and refined by least-squares on weighted F^2 values for all reflections.[35] All hydrogen atoms were constrained to ideal geometries and refined with isotropic displacement parameters equal to 1.2 times that of their parent atom. Refinement proceeded smoothly to give the residuals shown in Table 2. Complex neutral-atom scattering factors were used.[36] One and a half virtually identical but crystallographically independent molecules are present in the asymmetric unit of compound **5**. Elemental analyses were carried out by the Laboratory for Microanalysis, University of Bristol. Mass spectrometry analyses were carried out on a VG AutoSpec by the Mass Spectrometry Service, University of Bristol.

The salts $(LiC_5H_4)_2(CH_2)_2$ and $(LiC_5H_4)_2(CH_2)_3$ were prepared as described in the literature.[37] Commercial reagents $CoCl_2$, NH_4Cl, and $NaPF_6$ were used as supplied by Aldrich without further purification. Commercial solvents MeOH and CH_2Cl_2 were used as supplied by Fluka without further purification. Filter reagent aluminum oxide (activated, neutral, STD grade, ca. 150 mesh, 58 Å) was purchased from Aldrich and used as received.

The detailed experimental procedure presented here for the preparation of **5** is representative of that used for the preparation and isolation of the neutral and paramagnetic [*n*]cobaltocenophanes (n = 2, 3). The oxidation of neutral [*n*]cobaltocenophanes (n = 2, 3) in aqueous solution in the presence of NH_4Cl and atmospheric oxygen is presented in detail for compound **7** and is representative for the synthetic protocol for compounds **8** and **9**. Compounds **8** and **9** are isolated by means of phase precipitation of the corresponding [*n*]cobaltoceniumphane cation via addition of saturated aqueous solutions of $NaPF_6$. This procedure is described in detail for compound **8** and is representative for the preparation of **9**.

Synthesis of Co(η^5-C_5H_4)$_2$(CH_2)$_2$ (5). The flytrap ligand $(LiC_5H_4)_2(CH_2)_2$ (1.51 g, 8.88 mmol) and $CoCl_2$ (1.15 g, 8.88 mmol) were thoroughly mixed in the absence of solvent and cooled to −78 °C. At this temperature dry and degassed THF was added (200 mL) and the temperature maintained at −78 °C. The suspension was stirred for 16 h while allowed to warm to room temperature. After removal of all volatiles in vacuo, the black to purple residue was extracted with 3 × 50 mL of hexane and filtered to give a cherry red solution. Evaporation of all volatiles under reduced pressure left crude **5** as a dark black to purple microcrystalline solid. Purification via vacuum sublimation (40 °C/1.5 × 10^{-3} mbar) gave very dark red, single crystals suitable for X-ray analysis. Yield: 178 mg (0.827 mmol, 9%). Anal. Calc: C 67.00; H 5.62. Found: C 66.94; H 5.56. HR-MS (EI, 70 eV): 215.0271 (M^+, 100%, calcd mass for $C_{12}H_{12}{}^{59}Co$ 215.0271), 137 ($M^+ - C_5H_4$-CH_2, 85%), 72 (137 − C_5H_5, 45%).

Synthesis of Co(η^5-C_5H_4)$_2$(CH_2)$_3$ (6). From $(LiC_5H_4)_2(CH_2)_3$ (1.50 g, 8.15 mmol) and $CoCl_2$ (1.06 g, 8.16 mmol) 153 mg (0.668 mmol, 8% yield) of black single crystals suitable for X-ray analysis were isolated after vacuum sublimation (55 °C/1.5 × 10^{-3} mbar). Anal. Calc: C 68.13; H 6.16. Found: C 68.05; H 6.16. HR-MS (EI, 70 eV): 229.0427 (M^+, 100%, calcd mass for $C_{13}H_{14}{}^{59}Co$ 229.0428), 137 ($M^+ - C_5H_4$-CH_2CH_2, 15%).

Synthesis of [Co(η^5-C_5H_4)$_2$(CH_2)$_2$]Cl (7). After compound **5** (150 mg, 0.698 mmol) was suspended in H_2O (20 mL) NH_4Cl (700 mg, 13.1 mmol) was added. The reaction mixture was stirred for 16 h in the presence of atmospheric oxygen, until a bright orange solution was obtained. After filtration, the aqueous solution was evaporated to dryness and the remaining solids were extracted with 3 × 5 mL of CH_2Cl_2. All volatiles were removed under reduced pressure, and the remaining orange solid was dissolved in 2 mL of H_2O and filtered over Al_2O_3. After evaporation of all volatiles, **7** (140 mg, 0.558 mmol, 80% yield) was obtained as an orange solid. Single crystals of **7**·H_2O suitable for X-ray analysis were obtained from slow diffusion of hexanes into a saturated aqueous solution of **7** in CH_2Cl_2. Even after crystallization compound **7** was obtained only in ca. 97% purity as observed by ^{1}H NMR (^{1}H and ^{13}C{^{1}H} NMR spectra of compound **7** showing small resonances from unidentified impurities at high field and have been included in the Supporting Information).

^{1}H NMR (400 MHz) (d_2-methylene chloride): δ 3.77 (s, 4 H, C_2H_4), 5.92 (t, 4 H, η^5-C_5H_4), and 6.56 ppm (t, 4 H, η^5-C_5H_4). ^{13}C{^{1}H} NMR (100 MHz) (d_2-methylene chloride): δ 34.6 (C_2H_4), 84.6 and 87.4 (α and β η^5-C_5H_4), and 112.0 ppm (η^5-C_5H_4-C_{ipso}). HR-MS (ESI): 215.0262 (M^+, 100%, calcd mass for $[C_{12}H_{12}{}^{59}Co]^+$ 215.0271).

Synthesis of [Co(η^5-C_5H_4)$_2$(CH_2)$_2$][PF_6] (8). After compound **5** (150 mg, 0.698 mmol) was oxidized and filtered in a similar way to that described for compound **7**, a saturated, aqueous solution of $NaPF_6$ (4 mL) was added dropwise to precipitate **8** as a yellow solid, which was then washed with 5 mL of cold H_2O and 5 mL of cold Et_2O. Orange needles of **8** (203 mg, 0.564 mmol, 81% yield) could be obtained by diffusing hexanes into a saturated solution of **8** in CH_2Cl_2.

^{1}H NMR (400 MHz) (d_2-methylene chloride): δ 3.32 (s, 4 H, C_2H_4), 5.35 (t, 4 H, η^5-C_5H_4), and 6.37 ppm (t, 4 H, η^5-C_5H_4). ^{13}C{^{1}H} NMR (100 MHz) (d_5-pyridine): δ 33.7 (C_2H_4), 84.8 and 86.3 (α and β η^5-C_5H_4), and 110.8 ppm (η^5-C_5H_4-C_{ipso}). Anal. Calc: C 40.02; H 3.36. Found: C 40.54; H 3.83. HR-MS (EI, 70 eV): 215.0271 (M^+, 100%, calcd mass for $[C_{12}H_{12}{}^{59}Co]^+$ 215.0271), 137 ($M^+ - C_5H_4$-CH_2, 62%).

Synthesis of [Co(η^5-C_5H_4)$_2$(CH_2)$_3$][PF_6] (9). Compound **6** (150 mg, 0.654 mmol) was oxidized, filtered, washed, and dried as described for compound **8**. Compound **9** was obtained as a yellow solid. Recrystallization from MeOH yielded **9** as yellow needles (208 mg, 0.556 mmol, 85% yield).

^{1}H NMR (400 MHz) (d_5-pyridine): δ 1.84–1.86 (t, 4 H, C_3H_6), 2.01–1.96 (m, 2 H, C_3H_6), 5.48 (t, 4 H, η^5-C_5H_4), and 5.38 ppm (t, 4 H, η^5-C_5H_4). ^{13}C{^{1}H} NMR (100 MHz) (d_5-pyridine): δ 12.6 and 13.2 (C_3H_6), 83.5, 83.9, 84.6, 84.8, 84.9, and 85.1 (η^5-C_5H_4), and 103.7 ppm (η^5-C_5H_4-C_{ipso}). Anal. Calc: C 41.73; H 3.77. Found: C 42.29; H 3.83. HR-MS (EI, 70 eV): 229.0427 (M^+, 100%) (calcd mass for $[C_{13}H_{14}{}^{59}Co]^+$ 229.0427), 137 ($M^+ - C_5H_4$-CH_2, 10%).

Acknowledgment. The authors thank the EPSRC National Crystallography Service for collecting X-ray data for crystal

(34) Sheldrick, G. M. *SADABS*, version 2; University of Göttingen: Germany, 2003.

(35) *SHELXTL* program system version 6; Bruker AXS: Madison, WI, 2003.

(36) I*nternational Tables for Crystallography*; Kluwer: Dordrecht, 1992; Vol. C.

(37) Collins, S.; Hong, Y.; Taylor, N. J. *Organometallics* **1990**, *9*, 2695.

structure of **7**. U.M. thanks Ms. M. J. Lopez-Gomez for recording all cyclic voltammograms, and Dr. G. R. Whittell and D. E. Herbert for fruitful discussions. I.M. thanks the EU for a Marie Curie Chair and the RSC for a Wolfson Research Merit Award.

Supporting Information Available: X-ray crystallographic information for compounds **5**, **6**, and **7** in CIF format and ^{1}H and $^{13}C\{^{1}H\}$ NMR spectra for compounds **7** and **8** are available free of charge via the Internet at http://pubs.acs.org.

OM700941V